



Seasonal Cycle Biases in DGVM Simulations of Double-Cropping Systems: A Case Study in the Huang-Huai-Hai Plain

Shengjie Zhou¹, Tiexi Chen^{1,2}, Yingying Cui², Xin Chen², Shuci LIU³, Zhe Gu¹

¹School of Geographical Sciences, Nanjing University of Information Science and Technology, Nanjing 210044, Jiangsu, China

²Qinghai Provincial Key Laboratory of Plateau Climate Change and Corresponding Ecological and Environmental Effects, Qinghai University of Science and Technology, Xining 810016, China

³Department of Environment and Science, Queensland Government, Brisbane, QLD 4102, Australia

Correspondence to: Tiexi Chen (chentiexi@163.com)

Abstract. Global dynamic vegetation models (DGVMs) are essential tools for studying the changes in terrestrial ecosystems and their responses to climate change and human activities. However, these models exhibit substantial uncertainties when applied to croplands, particularly in regions with multiple cropping systems. These uncertainties arise from variations in planting types and phenology, which are influenced by sowing and harvesting schedules. This study focused on the phenological estimation errors of DGVMs in typical double - cropping agricultural regions. The Huang - Huai - Hai Plain in eastern China was chosen, which is one of the most important grain-producing areas with mainly winter wheat-summer crop rotation. A comparative analysis was conducted between the seven models from the TRENDY project and three remote sensing observations over last two decades. The results indicate that remote sensing vegetation indices consistently exhibit a typical bimodal structure in the study area, with peaks in April and August, corresponding to the growth peaks of the two-season crops. However, none of the DGVMs successfully capture this bimodal pattern. Given that multiple cropping systems are widespread in middle- and low-latitude regions with favorable water and temperature conditions, improving the simulation capabilities of DGVMs in such areas is an urgent and critical issue for advancing global vegetation modeling.

1 Introdution

Vegetation change, its attribution, and the feedback effects on climate are currently important topics of research. Terrestrial vegetation growth is highly sensitive to global changes (Houghton, 1995). Since the Industrial Revolution (Esau et al., 2016), various factors such as the increase in atmospheric carbon dioxide concentration (Keenan et al., 2013), climate warming (Xu et al., 2013; Lucht et al., 2002), enhanced nitrogen deposition (Penuelas et al., 2013), and land-use changes have significantly impacted the growth of terrestrial vegetation through complex biophysical and chemical processes (Lambin et al., 2001; Klein Goldewijk and Ramankutty, 2004). Therefore, globally, under the combined influence of natural and human activities, vegetation has shown a "greening" phenomenon, which refers to the statistically significant increase trend in vegetation greenness at an interannual scale (Piao et al., 2019). Vegetation changes have been primarily monitored through remote sensing, which provides relatively reliable long-term and large-scale observations. Remote sensing-derived vegetation indices, e.g., the



50



leaf area index (LAI)(Zhu et al., 2016), normalized difference vegetation index (NDVI)(Myneni et al., 1997) and enhanced vegetation index (EVI)(Huete et al., 2002) were widely used.

Both climate change and human activities have been investigated as driving forces behind greening processes. Notably, dynamic global vegetation models (DGVMs) have provided precise quantitative results (Schierhorn et al., 2013; Estel et al., 2015). A study analyzing the changing trends and driving factors of cumulative LAI during the global terrestrial growing season from 1982 to 2009, using remote sensing-based LAI time series and global vegetation dynamic models (Zhu et al., 2016), found that the cumulative LAI increase significantly across approximately 25 to 50% of the world's vegetated land, whereas less than 4% exhibited a notable decline. The same study further indicated that the rising atmospheric carbon dioxide concentration is the main driver of terrestrial vegetation change (70%), followed by nitrogen deposition (9%), climate change (8%) and land use (4%). The CO₂ fertilization effect is most evident in tropical areas (Ahlström et al., 2015).

However, managed lands—particularly croplands—have been shown by observations to make a substantial contribution to global greening, challenging the conclusion from DGVMs that attributes this trend primarily to the CO₂ fertilization effect. In addition, China's greening is primarily observed in forests (42%) and cropland (32%), while India's greening is largely driven by croplands (82%), with a smaller contribution from forests (4.4%)(Chen et al., 2019). This highlights the critical need to rigorously evaluate and improve DGVMs' capacity to simulate agricultural systems.

To effectively study vegetation dynamics, it is essential to first validate that Dynamic Global Vegetation Models (DGVMs) can accurately capture the fundamental seasonal characteristics of vegetation, particularly its phenological aspects. Phenology changes, including the advancement of the start of the growing season (SOS), the delay of the end of the growing season (EOS), and the enhancement of peak greenness, can significantly alter the Earth's seasonal landscape. Vegetation can adapt to climate change through relatively fast mechanisms, such as phenological or physiological adjustments. By modifying the growing season and phenology, global warming is expected to increase the productivity of northern ecosystems(Huang et al., 2017). Compared to natural vegetation, cropland vegetation differs significantly, particularly because agricultural activities give rise to unique phenological traits. This is especially evident in regions with high-intensity agriculture—namely, double-cropped

Multiple cropping is common and widespread land-use management strategy in low-land tropical and subtropical agriculture where rainy seasons are long enough or irrigation is viable. Changes in cropping intensity, not just in harvested area and crop yields are associated with crop production. Research indicates that multiple cropping systems cover 135 million hectares (12% of global cropland), with 85 million hectares in irrigated agriculture. About 34%, 13%, and 10% of the rice, wheat, and maize areas, respectively, are under multiple cropping systems, underscoring the importance of these systems for cereal production (Waha et al., 2020).

farmlands—which exhibit phenological characteristics that are markedly different from those of natural vegetation.

Intensifying multiple cropping is considered an important means of increasing food production without expanding cropland area(Wu et al., 2018). However, processes related to multiple cropping are rarely represented in current DGVMs. Cropping intensity is generally expressed on a scale of 1-3, corresponding to single, double, and triple cropping, respectively. Yet, because multiple cropping systems are often complex and interspersed with intermittent fallow periods, many such areas are



75

80



not stably cultivated over long timescales(Waha et al., 2025). In light of this, we selected the Huang-Huai-Hai Plain, a highly representative double-cropping region, as our study area. Since the 1980s, this region has been dominated by a winter wheat—summer crop double-cropping system. The objective of this study is to highlight the significant limitations that remain in current DGVMs with respect to accurately simulating the vegetation seasonality driven by intensively managed double-cropping systems.

2 Data and Methods

2.1 Study Area

The Huang-Huai-Hai Plain, formed by the alluvial deposits of the Yellow River, Huaihe River, Haihe River, and their tributaries, is located in eastern China. It lies within the warm temperate continental monsoon climate zone, covering area between 31°N–43°N and 112°E–124°E. The topography is illustrated in Fig.1a, using Global 15 Arc-Second Elevation (Weatherall et al., 2024). While plains dominate the area, there are also several mountainous regions, including Mount Tai in Shandong Province, and the Taihang and Yan Mountains on the western edge of Hebei Province. The North China Plain (NCP) is one of the most significant agricultural regions in China, encompassing approximately 18 million hectares of farmland, or 18.3% of the national total. The double-cropping system of winter wheat and summer maize, named for the seasons in which they are planted, accounts for 60% of the arable land in this area.(Sun et al., 2007)

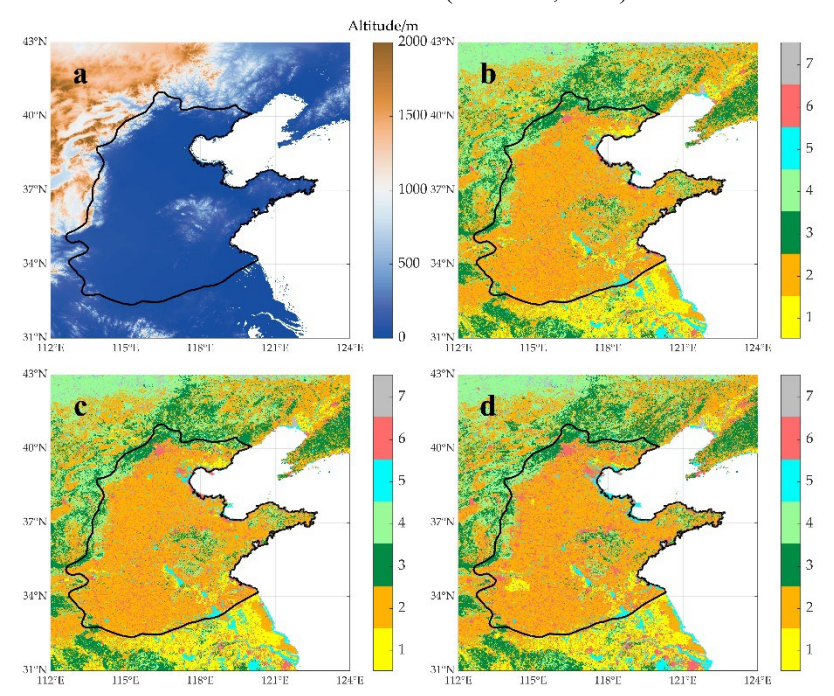


Figure 1: The location of Huang-Huai-Hai Plain and its land cover types. a) Location of the study plain and its topography. b-d) Land cover types of 3 years of 2000, 2015 and 2020 based on RESDC data at xx resolution. The land use types represented by serial

https://doi.org/10.5194/egusphere-2025-4997 Preprint. Discussion started: 19 November 2025

© Author(s) 2025. CC BY 4.0 License.





numbers 1-7 are Paddy cropland, dry cropland, woodland, grassland, water body, build land, unused land. More detail of the Land cover types and changes is listed in Table 1.

2.2 Dataset

85

100

In this study, LAI was employed to characterize vegetation conditions due to its well-defined ecological significance and extensive utilization in global greening research. Monthly LAI datasets simulated by seven DGVMs from the TRENDY project (Sitch et al., 2024) with a spatial resolution of 0.5 degrees are selected for analysis.

To complement the model simulations and reflect real-world vegetation conditions, three remote-sensing-derived LAI datasets were also incorporated. The 8-day 500 m resolution MODIS LAI (MOD15A2H, Version 6.1)(Myneni et al., 2021) were obtained from the LAADS DAAC (Level-1B and Atmosphere Archive & Distribution System Distributed Active Archive Center).

The GLASS (The Global Land Surface Satellite) LAI dataset (version V60)(Ma and Liang, 2022), featuring an 8-day temporal resolution and 0.05 degrees spatial resolution, was developed using a bidirectional long short-term memory (BiLSTM) machine learning model applied to MODIS observations.

The Global Inventory Modeling and Mapping Studies (GIMMS) LAI4g dataset, spanning 1982-2020, was generated by integrating AVHRR data (1982-2003) and reprocessed MODIS LAI (2004-2020) through a backpropagation neural network (BPNN) and data consolidation method (Zhu et al., 2023)24. This dataset provides a spatial resolution of 1/12th degrees and a semi-monthly temporal resolution.

To ensure consistency in comparative analysis with DGVM outputs, all LAI datasets were standardized to a common temporal coverage (2001-2023), spatial resolution (0.5 degrees), and monthly temporal resolution. Detailed dataset parameters are summarized in Table 2.

The land-cover dataset (Fig. 1b-d) sourced from the Data Center for Resources and Environmental Sciences, Chinese Academy of Sciences (RESDC) (https://www.resdc.cn) provides a 1 km spatial resolution(徐新良 et al., 2018). Derived from Landsat imagery, this dataset categorizes land into six primary land use/land cover classes, with proportional distributions detailed in Table 1. A notable characteristic is the explicit separation of paddy fields and dry fields within the cropland category. This distinction facilitates a clear assessment of the prevalence of double-cropping systems in the study area and confirms that cropping systems and planting areas remained relatively stable throughout the research period.

110 2.3 Seasonal cycle and trend analysis

Given that the Huang-Huai-Hai Plain is a typical double-cropping agricultural region, two spatial masks—one for cropland and the other for natural vegetation (including grassland and woodland)—were constructed to analyse statistical differences between artificially managed and unmanaged land.





The Mann-Kendall test was applied to assess the significance of temporal trends in the variables. The coefficient of determination (R²) and F-test were used to evaluate the goodness-of-fit of linear regressions and their corresponding statistical significance.

3 Results

120

125

3.1 Annual LAI spatial pattern and regional average inter-annual trends

We first evaluated the spatial distribution of the multi-year mean LAI (Fig.2). The results from the remote-sensing datasets are largely consistent, showing denser vegetation cover in the southwest, where the mid-latitude monsoon climate brings higher temperatures and precipitation compared with the north, creating more favorable conditions for vegetation growth. By contrast, the TRENDY simulations only partly reproduce this north-south gradient, while exhibiting more pronounced spatial discrepancies in LAI magnitude. Four of the seven models substantially overestimate LAI values. Whereas the three remote-sensing products report a maximum annual mean LAI of around 2 at the 0.5° grid scale, some model outputs exceed 5, indicating a significant overestimation of vegetation density. Among the models, LPJ-GUESS shows the closest agreement with remote-sensing datasets in terms of both mean values and spatial patterns.

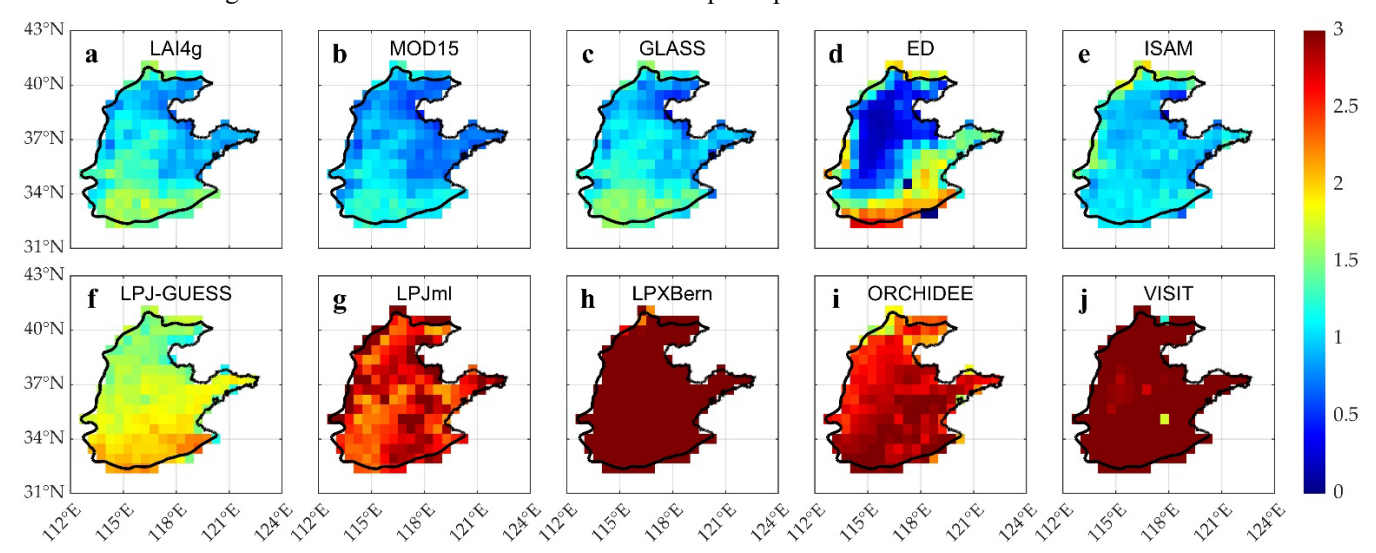


Figure 2: The spatial distribution of average annual LAI of Huang-Huai-Hai Plain. Fig.2a-j respectively represents LAI4g, MOD15, GLASS, ED, ISAM, LPJ-GUESS, LPJml, LPXBern, ORCHIDEE and VISIT.

130 Regional mean values are shown in Fig.3a. The three remote-sensing datasets are broadly consistent, while DGVMs yield considerably higher estimates, in some cases exceeding the observational values by more than fourfold. In terms of magnitude comparisons, remote-sensing-derived LAI shows only minor differences between cropland and natural vegetation, with mean annual values stabilizing around 1. DGVMs, however, apply different parameterizations for cropland and natural vegetation, resulting in divergent LAI ranges. For instance, models such as ED, ISAM, LPJml, and VISIT predict higher LAI in natural



145

150



vegetation, whereas LPJ-GUESS, LPXBern, and ORCHIDEE estimate greater LAI in croplands. These findings suggest that DGVMs still exhibit substantial uncertainties in simulating vegetation distribution in cropland areas.

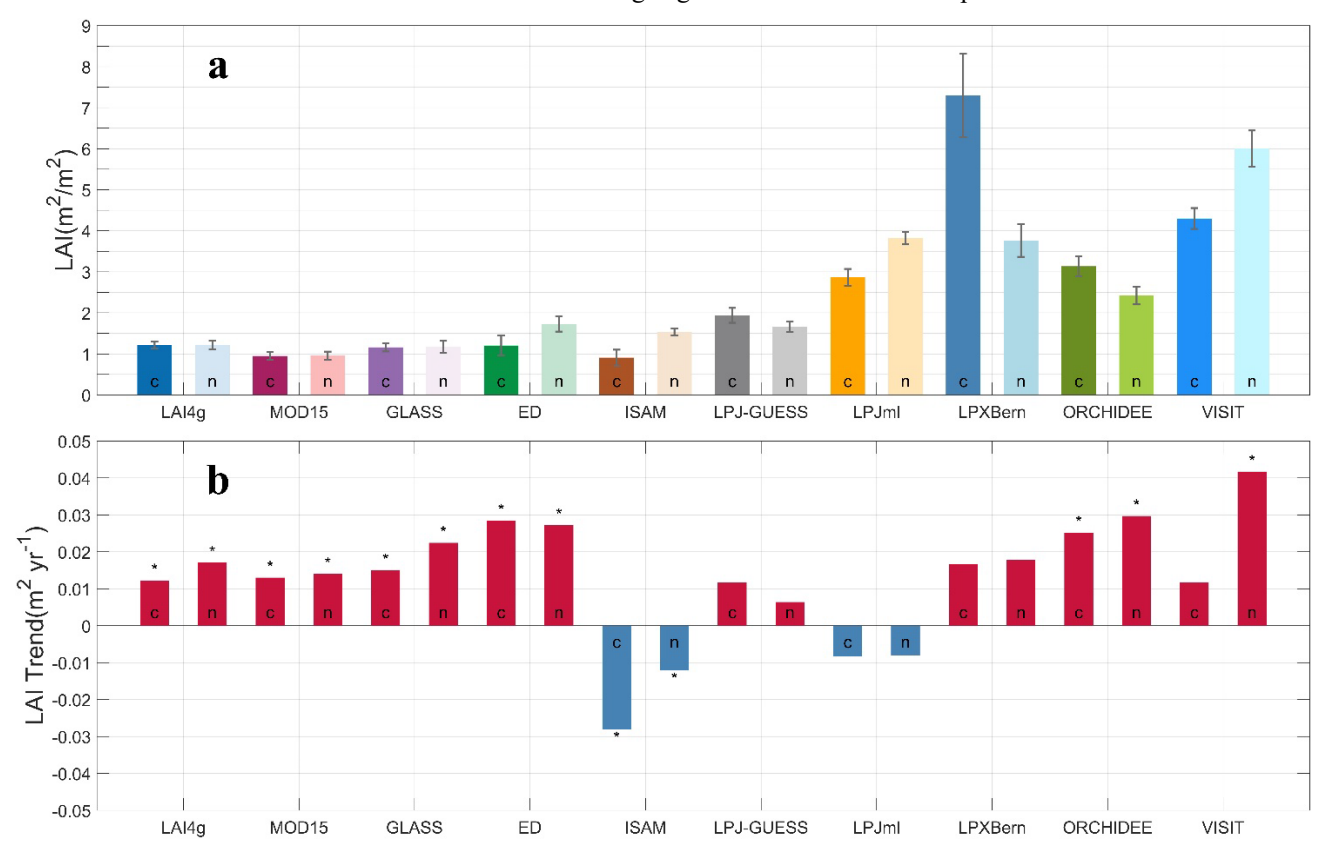


Figure 3: Average annual LAI and linear fitting trends of LAI of cropland and natural vegetation. a) the height of the bar graph represents the average annual LAI value and the error bar represents plus or minus one standard deviation. The dark colors with 'c' on left represent the cropland and the light colours with 'n' on right represent the natural vegetation. b) the height of the bar graph represents linear trend of average annual LAI, Red represents a positive trend and blue represents a negative trend; The asterisk(*) on the top of bar means the linear trend pass the significance test(p < 0.05).

Long-term vegetation dynamics represent another key indicator. With rising atmospheric CO₂ concentrations, ecosystems—absent disturbances such as extreme climate events—tend to exhibit enhanced canopy greenness, reflected as multi-year increases in vegetation indices or LAI. In this region, all three remote-sensing datasets reveal a significant greening trend across both croplands and natural vegetation. Notably, natural vegetation shows slightly higher LAI increase rates: LAI4g (0.0171 yr⁻¹), MOD15 (0.0141 yr⁻¹), and GLASS (0.0224 yr⁻¹), compared with croplands: LAI4g (0.0123 yr⁻¹), MOD15 (0.0130 yr⁻¹), and GLASS (0.0151 yr⁻¹). By contrast, although most models also simulate an increasing LAI trend in this region, ISAM and LPJml instead produce declining trends, which is clearly inconsistent with observations.

The spatial distribution of long-term trends is shown in Fig.4. All three remote-sensing datasets consistently reveal a greening pattern, both in terms of spatial extent and magnitude (Fig.4a-c). In contrast, ISAM produces a widespread declining trend, clearly differing from the other DGVMs, while LPX-Bern substantially overestimates the greening magnitude. In the linear





160

165

trend analysis, the remote-sensing datasets consistently indicate steady greening, whereas DGVMs show substantial divergence in both magnitude and direction, underscoring persistent model biases in capturing long-term vegetation changes.

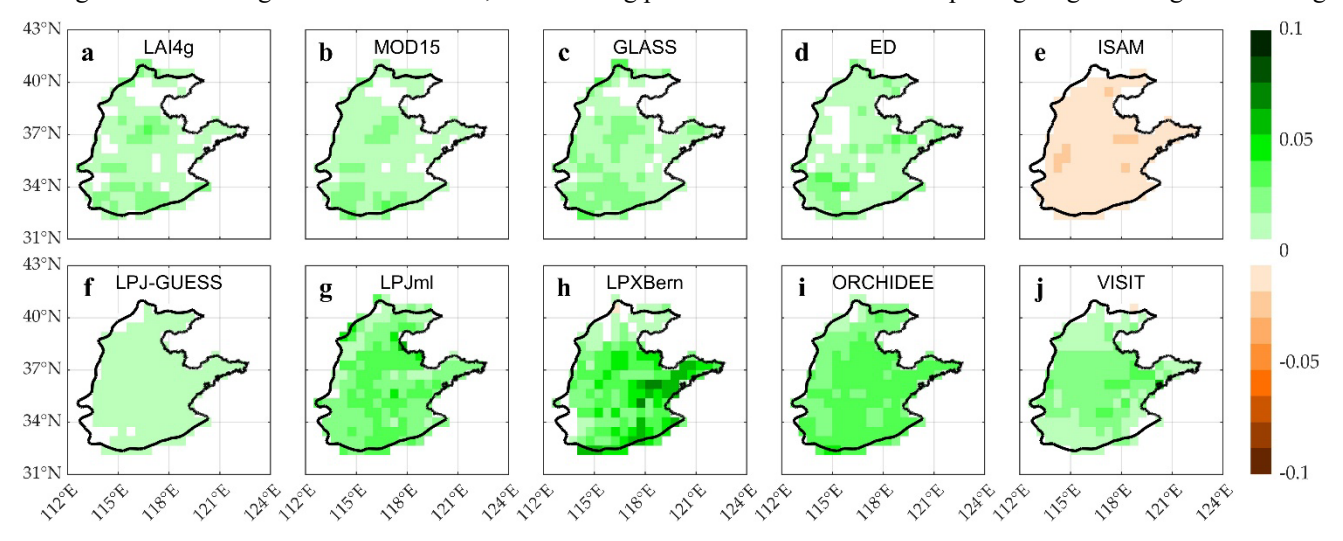


Figure 4: The spatial distribution of annual LAI linear fitting trends of Huang-Huai-Hai Plain. Fig.2a-j respectively represents LAI4g, MOD15, GLASS, ED, ISAM, LPJ-GUESS, LPJml, LPXBern, ORCHIDEE and VISIT.

3.2 Seasonal patterns comparison

The phenology of double-cropping farmlands differs markedly from that of natural vegetation, exhibiting two biological cycles within a single year. While phenological studies often characterize vegetation dynamics using indicators such as the start, end, and length of the growing season, our focus here is on broader temporal patterns—specifically, whether current DGVMs capture the fundamental bimodal pattern of LAI. In this study, the Huang-Huai-Hai Plain serves as a representative double-cropping region in China, dominated by a winter wheat–summer crop rotation system. Winter wheat is typically sown in early October and harvested in early June of the following year, a schedule that is relatively fixed given the limited alternatives for overwintering field crops. By contrast, summer crops—such as maize, soybean, or cotton—are sown immediately after the wheat harvest and mature by late September. This sequential cropping system results in two distinct seasonal peaks in monthly LAI, occurring in April and August and corresponding to the peak growth phases of the two crops (Fig.5a1-c1). All remotesensing vegetation indices consistently confirm this bimodal pattern. Furthermore, two sharp declines in LAI are observed around June and October, coinciding with the harvest periods.



180

185



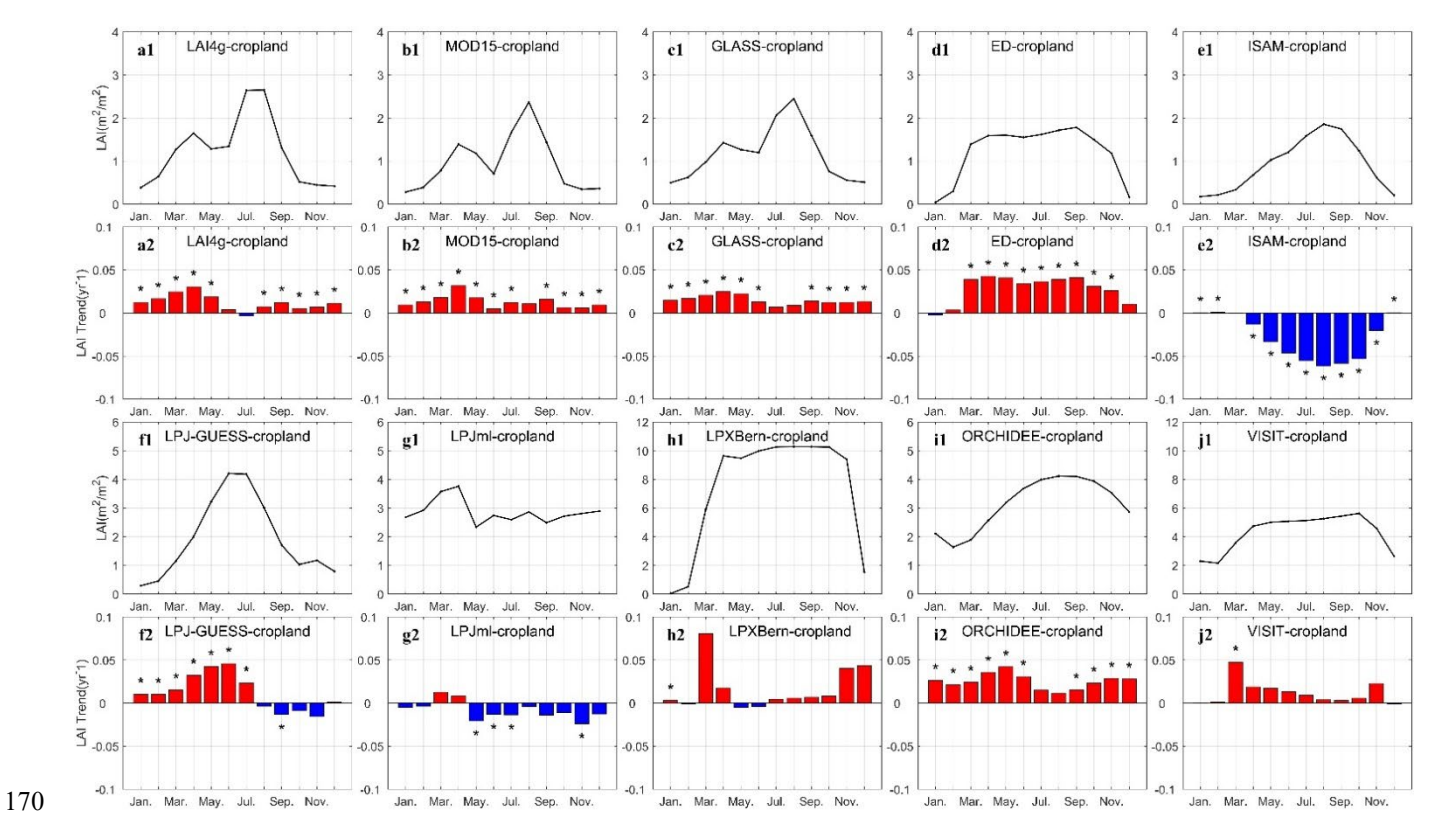


Figure 5: Seasonal cycles and linear fitting trends of monthly LAI for cropland. The dataset names are abbreviated in the subheading; The line graph represents the monthly average of LAI and the bar graph represents linear trend of average monthly LAI, Red represents a positive trend and blue represents a negative trend; The asterisk(*) on the top of bar means the linear trend pass the significance test(p <0.05).

By contrast, none of the dynamic global vegetation models (DGVMs) successfully reproduce the bimodal LAI structure of croplands, indicating that current model frameworks do not adequately represent multiple cropping systems. Moreover, the simulated seasonal patterns of cropland LAI differ considerably across models, which can be broadly grouped into three types. The first type, exemplified by ISAM, LPJ-GUESS, and ORCHIDEE, shows a single summer peak lasting only 1–2 months, with LAI gradually increasing from its winter minimum. The second type, represented by ED, LPX-Bern, and VISIT, is characterized by rapid increases and decreases in LAI during spring and autumn, with an extended high-LAI period during the summer half-year (exceeding five months). The third type, as in LPJml, displays a maximum LAI in late spring. These differences reflect contrasting representations of cropland vegetation characteristics among models. Compared with remotesensing observations, it is evident that current DGVMs fail to capture the phenology of double-cropping systems.

For comparison with cropland vegetation, we further extracted LAI data for natural vegetation (Fig.6). Unlike the bimodal structure observed in croplands, remotely sensed LAI of natural vegetation exhibits a unimodal seasonal pattern, closely





aligned with variations in hydrothermal conditions, with the peak typically occurring between July and August. By contrast, the simulations retain a bimodal structure similar to that of croplands. It is also noteworthy that the simulated differences between cropland and natural vegetation are far less pronounced than those indicated by remote-sensing observations.

A direct comparison of the two seasonal cycle plots in Fig.S2 renders the results more evident: LAI growth rates simulated by the ED model decline during mid-year, corroborating our earlier hypothesis. Another key observation is that, from January to April, cropland LAIs consistently exceed those of natural vegetation in remote-sensing datasets (Fig.S2a,S2b,S2c). We attribute this to anthropogenic management practices—including sowing, irrigation, and fertilization—that accelerate the growth cycle of winter wheat, leading to its peak to occur earlier than that of natural vegetation. Simulated datasets, however, do not align with this finding.

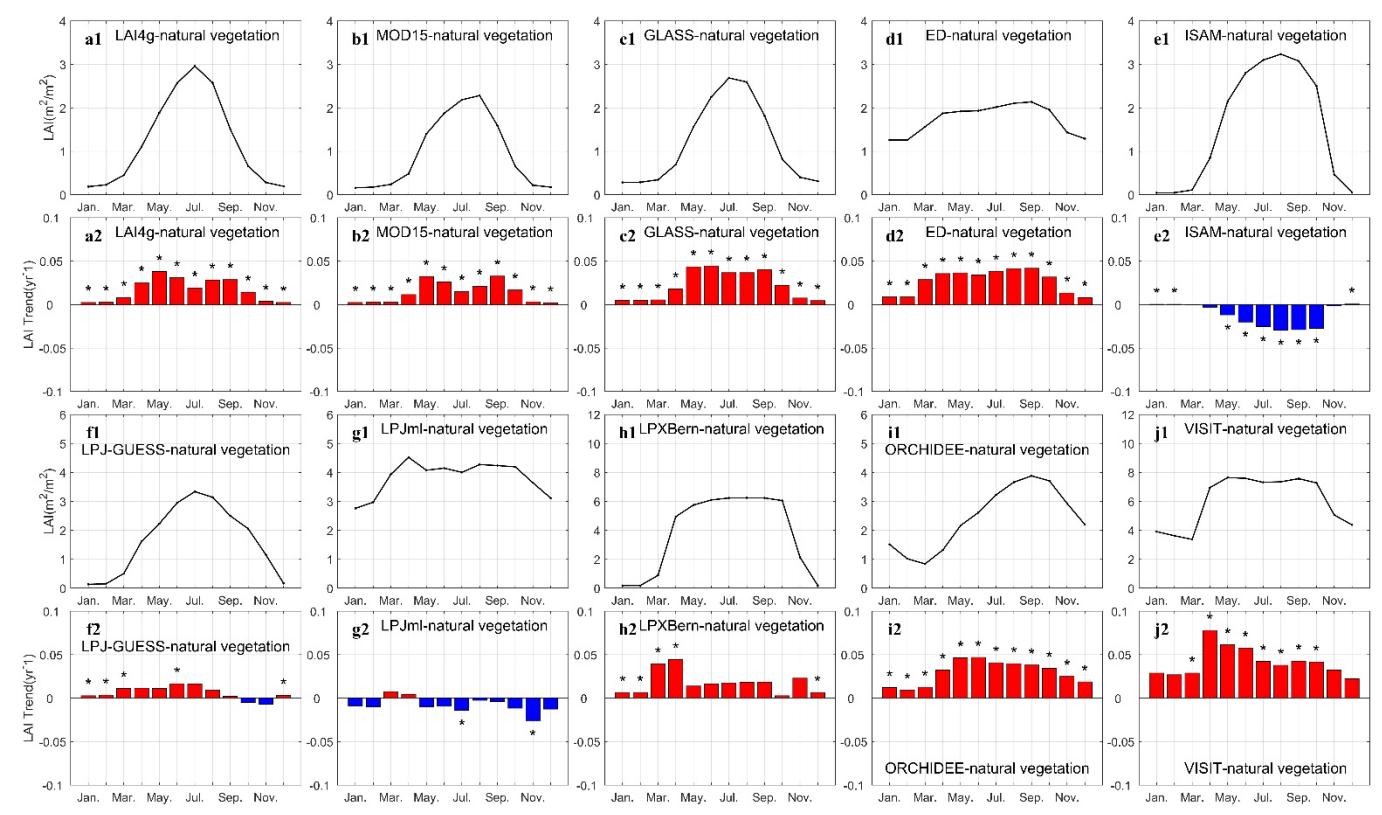


Figure 6: Seasonal cycles and linear fitting trends of monthly LAI for natural vegetation. The dataset names are abbreviated in the subheading; The line graph represents the monthly average of LAI and the bar graph represents linear trend of average monthly LAI, Red represents a positive trend and blue represents a negative trend; The asterisk (*) on the top of bar means the linear trend pass the significance test (p <0.05).

3.2 Inter-annual trends over different months

200

Seasonal differences are reflected not only in the climatological seasonal cycle but also in the month-to-month variations in long-term trends. For croplands, the monthly LAI linear trends from remote-sensing datasets show a persistent greening signal in nearly all months (except July in MOD15), particularly during the first half of the year (Fig.4). The strongest increases occur





- in April—May, coinciding with the peak growth of winter wheat, whereas trends in the second cropping season are comparatively weaker. For natural vegetation, greening is concentrated in the latter half of the year (April—September), with a reduced signal in July, likely due to mixed pixels containing croplands and natural vegetation. Overall, natural vegetation exhibits slightly higher long-term LAI growth rates than croplands.
- To further examine seasonal characteristics of long-term changes, we divided the year according to the double-cropping system:

 spring growing season (SGS, March–May), summer sowing/transition season (SSS, June–July), autumn growing season (AGS, August–October), and winter season (WS, November–February). The spatial distribution of monthly LAI linear trends derived from remote sensing (Fig.7) reveals that croplands show the strongest greening during SGS. The greening signal diminishes during the transition period, weakens further in AGS, and remains marginal but positive during WS. In contrast, DGVMs fail to reproduce these seasonal features and in some cases even show opposite trend directions.
- 215 Taken together, DGVM-simulated vegetation indices do not accurately capture vegetation dynamics in the Huang-Huai-Hai Plain, particularly in cropland regions. Three main issues stand out: (1) models tend to overestimate absolute LAI values; (2) they fail to represent the seasonal dynamics of the double-cropping system, especially the timing and intensity of growth stages; and (3) they underestimate the contribution of croplands to the regional greening trend.
- Overall, the simulated vegetation indexes from DGVMs may not capture the actual vegetation condition in the Huang-Huai220 Hai Plain, particularly for cropland. It is mainly reflected in three points. First, DGVMs tend to overestimate the overall magnitude of LAI. Second, they fail to accurately reproduce the seasonal dynamics of double-cropping systems, especially the timing and intensity of growth phases. Third, they underestimate the contribution of cropland to regional greening trends.

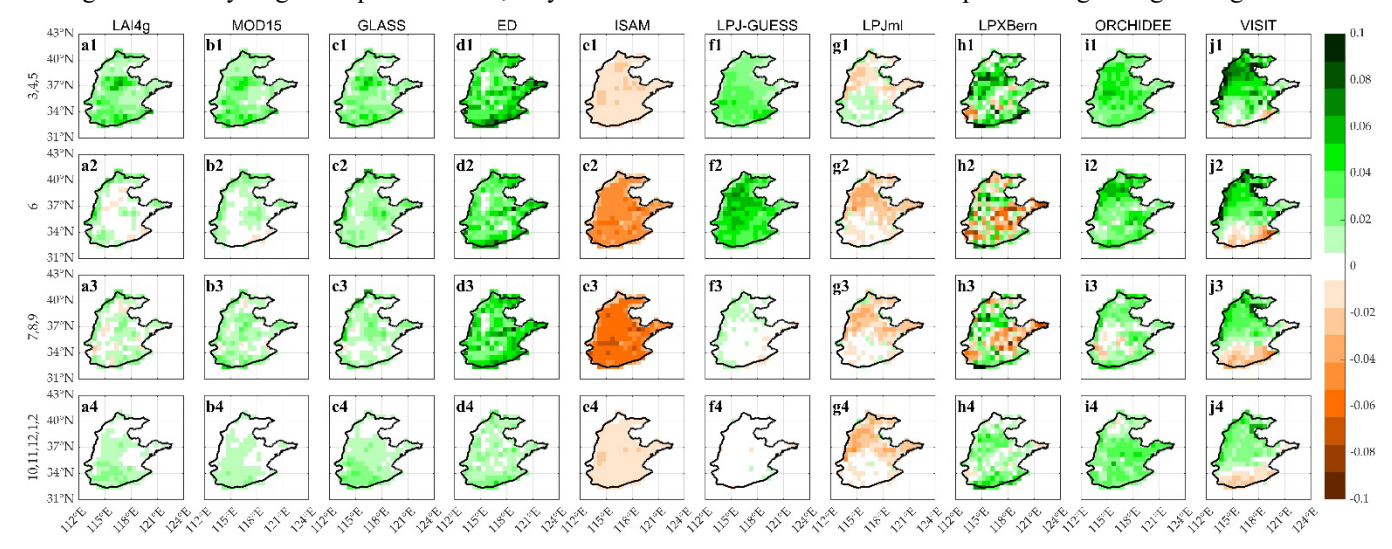


Figure 7: The spatial distribution of time division LAI linear trends of Huang-Huai-Hai Plain. Divide the year into four periods, The whole year is divided into four periods, corresponding to the four periods of cropland. The 3rd,4th,5th months corresponding to the rapid growth period of wheat; The 6th,7th months corresponding to the period of wheat harvest and corn sowing; The 8th,9th,10th months corresponding to the growth period of corn and harvest; The 11th,12th,1st,2nd months corresponding to the winter period of wheat.





4 Discussion

- Dynamic global vegetation models (DGVMs) are widely used to assess ecosystem responses to climate change(Prentice et al., 2007), and most land surface models embedded within Earth system models now include such capabilities(Martín Belda et al., 2022; Lawrence et al., 2019). However, their ability to simulate human-managed land cover remains limited, particularly for urban green spaces and croplands. Under climate warming, intensifying cultivation to increase food production has become an important strategy, with double-cropping systems being one of the most representative examples.
- In this study, we focus on the Huang-Huai-Hai Plain, one of the world's longest-standing double-cropping regions, to systematically analyze the seasonal characteristics and long-term dynamics of vegetation. Comparison with multiple DGVM simulations reveals substantial biases in both the representation of double-cropping seasonal cycles and long-term greening trends, highlighting the urgent need to improve model performance in such agricultural regions.
- Previous research has shown that approximately 70% of the global greening trend can be attributed to the CO₂ fertilization effect(Zhu et al., 2016). More recent analyses emphasize the significant contribution of croplands to greening, while pointing to the need for improved representation of human land-use practices in models(Chen et al., 2019). Mathison et al. used the JULES land surface model to simulate multi-season crop rotations at sites in France and India, thereby improving the accuracy of carbon and energy fluxes during secondary crop growing seasons(Mathison et al., 2021).
- 245 parameter optimization; and (3) the precision of input driver datasets. The Huang-Huai-Hai case study demonstrates that simulated vegetation indices differ significantly from satellite-based observations, particularly in the amplitude and characteristics of seasonal cycles. This discrepancy arises because current DGVMs lack explicit mechanisms for double-cropping systems. Inappropriate parameterizations may also lead to systematic overestimation of grid-scale LAI values. Moreover, the TRENDY project employs the HYDE global historical environment database(Klein Goldewijk et al., 2017) as a proxy for cropland dynamics. Yet, while global products are useful at large scales, regional-scale land use/cover change (LUCC) datasets are often more accurate. The RESDC LUCC dataset, derived from remote sensing and validated at local scales, provides a more realistic representation of land cover in the Huang-Huai-Hai Plain. A comparison of HYDE3.3 and RESDC (Fig.8) shows that HYDE unrealistically exaggerates interannual variability in cropland area, despite the relative stability of land use in this region, and that its spatial distribution of croplands deviates from actual conditions.
- Although remote-sensing data provide consistent and robust evidence, the assumption that each 0.5° grid cell represents a homogeneous land cover type introduces additional uncertainty, since these grid cells often contain mixed land uses, with croplands occupying only part of the area. This assumption may obscure the seasonal dynamics of croplands in model simulations.
- To improve the accuracy and applicability of DGVMs, future research should extend analyses to larger regions to investigate double-cropping and fallow systems at the global scale, with a particular focus on three priorities: (1) incorporating explicit



270

280

285



mechanisms for cropping systems; (2) optimizing regional parameterizations; and (3) integrating locally validated LUCC and crop calendar datasets.

Further improvements will also require more accurate information on cropping intensity. For future projections, such estimates must account for both climate change and socioeconomic development to provide realistic scenarios of cultivation intensity. In addition, modeling must better reflect crop-specific characteristics: winter—spring crops are typically dominated by winter wheat, whereas summer crops vary more widely (e.g., maize, soybean, cotton), although their seasonal cycles are relatively well defined.

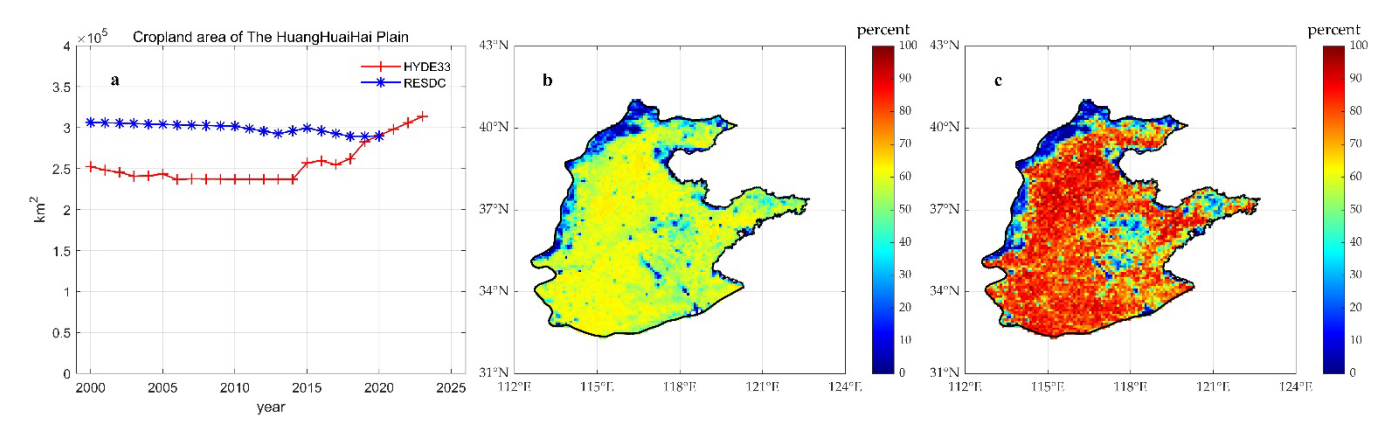


Figure 8: Total area and distribution of cropland of the Huang-Huai-Hai Plain. a) Annual total cropland area b) Coverage ratio of cropland from HYDE3.3 in 2010 c) Coverage ratio of cropland from RESDC in 2010.

5 Conclusions

By integrating satellite observations with dynamic global vegetation model (DGVM) simulations of leaf area index (LAI), this study systematically evaluated vegetation growth dynamics in the Huang-Huai-Hai Plain. The results highlight three major limitations of current DGVMs in representing the double-cropping agricultural system:

First, DGVMs systematically overestimate LAI values. In some cases, simulated values far exceed the observational range. For example, satellite-based estimates at the 0.5° grid scale show an annual maximum mean LAI of around 2, whereas several DGVMs produce values greater than 5. Such discrepancies can lead to misinterpretations of vegetation cover and productivity in double-cropping regions.

Second, DGVMs fail to capture the seasonal dynamics of double-cropping systems. Remote-sensing observations reveal a characteristic bimodal LAI structure in the Huang-Huai-Hai Plain, with peaks in April (winter wheat) and August (summer maize). However, none of the seven DGVMs included in the TRENDY project reproduce this seasonal pattern. This deficiency constrains the models' predictive ability for crop-related ecological processes, including carbon cycling and water balance. Third, DGVMs underestimate the contribution of croplands to regional greening trends. Satellite observations clearly identify croplands as the dominant driver of greening in the Huang-Huai-Hai Plain, yet DGVM outputs diverge substantially from observations in both spatial patterns and temporal dynamics.



290



Improving DGVM representation of double-cropping systems is therefore critical for enhancing the predictive accuracy of global change models. Future research should prioritize: (1) embedding explicit mechanisms of double-cropping into model structures; (2) optimizing parameterizations at regional scales; and (3) incorporating high-resolution, locally validated datasets on land use, cropping systems, and phenology. These advances will substantially improve the ability of DGVMs to simulate the complex interactions among human activities, agricultural systems, and terrestrial ecosystems under global environmental change.

Data availability. Leaf Area Index data from GIMMS-LAI4g is available at https://zenodo.org/records/8281930; MOD15A2H can be achieved from https://www.earthdata.nasa.gov/data/catalog/lpcloud-mod15a2h-061; Leaf Area Index data from GLASS can be downloaded at https://glass.hku.hk/download.html; TRENDY-v12 datasets are available from the following website: https://globalcarbonbudgetdata.org/; Land cover types based on RESDC data is available at https://www.resdc.cn/.

Author contributions. TC conceived the scientific ideas and designed this research framework. SZ compiled the data, conducted analysis, and prepared figures. SZ, TC, and SL wrote the article. YC, ZG, and XC gave constructive suggestions for improving the article.

Competing interests. The contact author has declared that none of the authors has any competing interests.

Acknowledgements. We acknowledge the Global Carbon Project, which is responsible for the Global Carbon Budget and we thank the land modelling groups for producing and making available their model output.

Financial support. This study was supported by the Natural Science Foundation of Qinghai Province (grant no. 2023-QLGKLYCZX-023), the National Natural Science Foundation of China (grant nos. 42130506, 42161144003, and 31570464).

References

- Ahlström, A., Raupach, M. R., Schurgers, G., Smith, B., Arneth, A., Jung, M., Reichstein, M., Canadell, J. G., Friedlingstein, P., and Jain, A. K.: The dominant role of semi-arid ecosystems in the trend and variability of the land CO₂ sink, *Science*, 348, 895–899, https://doi.org/10.1126/science.aaa1668, 2015.
 - Chen, C., Park, T., Wang, X., Piao, S., Xu, B., Chaturvedi, R. K., Fuchs, R., Brovkin, V., Ciais, P., Fensholt, R., Tømmervik, H., Bala, G., Zhu, Z., Nemani, R. R., and Myneni, R. B.: China and India lead in greening of the world through land-use management, *Nat. Sustain.*, 2, 122–129, https://doi.org/10.1038/s41893-019-0220-7, 2019.
- Esau, I., Miles, V. V., Davy, R., Miles, M. W., and Kurchatova, A.: Trends in normalized difference vegetation index (NDVI) associated with urban development in northern West Siberia, *Atmos. Chem. Phys.*, 16, 9563–9577, https://doi.org/10.5194/acp-16-9563-2016, 2016.
- Estel, S., Kuemmerle, T., Alcántara, C., Levers, C., Prishchepov, A., and Hostert, P.: Mapping farmland abandonment and recultivation across Europe using MODIS NDVI time series, *Remote Sens. Environ.*, 163, 312–325, https://doi.org/10.1016/j.rse.2015.03.028, 2015.





- Houghton, R. A.: Land-use change and the carbon cycle, *Glob. Change Biol.*, 1, 275–287, https://doi.org/10.1111/j.1365-2486.1995.tb00026.x, 1995.
- Huang, M., Piao, S., Janssens, I. A., Zhu, Z., Wang, T., Wu, D., Ciais, P., Myneni, R. B., Peaucelle, M., Peng, S., Yang, H., and Peñuelas, J.: Velocity of change in vegetation productivity over northern high latitudes, *Nat. Ecol. Evol.*, 1, 1649–1654, https://doi.org/10.1038/s41559-017-0328-y, 2017.
 - Huete, A., Didan, K., Miura, T., Rodriguez, E. P., Gao, X., and Ferreira, L. G.: Overview of the radiometric and biophysical performance of the MODIS vegetation indices, *Remote Sens. Environ.*, 83, 195–213, https://doi.org/10.1016/S0034-4257(02)00096-2, 2002.
- 330 Keenan, T. F., Hollinger, D. Y., Bohrer, G., Dragoni, D., Munger, J. W., Schmid, H. P., and Richardson, A. D.: Increase in forest water-use efficiency as atmospheric carbon dioxide concentrations rise, *Nature*, 499, 324–327, https://doi.org/10.1038/nature12291, 2013.
 - Klein Goldewijk, K. and Ramankutty, N.: Land cover change over the last three centuries due to human activities: The availability of new global data sets, *Glob. Biogeochem. Cycles*, 18, GB335, https://doi.org/10.1029/2004GB002315, 2004.
- Klein Goldewijk, K., Beusen, A., Doelman, J., and Stehfest, E.: Anthropogenic land use estimates for the Holocene HYDE 3.2, Earth Syst. Sci. Data, 9, 927–953, https://doi.org/10.5194/essd-9-927-2017, 2017.
 Lambin, E. F., Turner, B. L., Geist, H. J., Agbola, S. B., Angelsen, A., Bruce, J. W., Coomes, O. T., Dirzo, R., Fischer, G., and Folke, C.: The causes of land-use and land-cover change: Moving beyond the myths, Glob. Environ. Change, 11, 261–269, https://doi.org/10.1016/S0959-3780(01)00007-3, 2001.
- Lawrence, D. M., Fisher, R. A., Koven, C. D., Oleson, K. W., Swenson, S. C., Bonan, G., Collier, N., Ghimire, B., Van Kampenhout, L., and Kennedy, D.: The Community Land Model version 5: Description of new features, benchmarking, and impact of forcing uncertainty, *J. Adv. Model. Earth Syst.*, 11, 4245–4287, https://doi.org/10.1029/2018MS001583, 2019.
 Lucht, W., Prentice, I. C., Myneni, R. B., Sitch, S., Friedlingstein, P., Cramer, W., Bousquet, P., Buermann, W., and Smith, B.: Climatic control of the high-latitude vegetation greening trend and Pinatubo effect, *Science*, 296, 1687–1689,
- 345 https://doi.org/10.1126/science.1071828, 2002.
 Ma, H. and Liang, S.: Development of the GLASS 250 m leaf area index product (version 6) from MODIS data using the bidirectional LSTM deep learning model, *Remote Sens. Environ.*, 273, 112985, https://doi.org/10.1016/j.rse.2022.112985, 2022.
 - Martín Belda, D., Anthoni, P., Wårlind, D., Olin, S., Schurgers, G., Tang, J., Smith, B., and Arneth, A.: LPJ-
- 350 GUESS/LSMv1.0: A next-generation land surface model with high ecological realism, *Geosci. Model Dev.*, 15, 6709–6745, https://doi.org/10.5194/gmd-15-6709-2022, 2022.
 - Mathison, C., Challinor, A. J., Deva, C., Falloon, P., Garrigues, S., Moulin, S., Williams, K., and Wiltshire, A.: Implementation of sequential cropping into JULESvn5.2 land-surface model, *Geosci. Model Dev.*, 14, 437–471, https://doi.org/10.5194/gmd-14-437-2021, 2021.
- Myneni, R., Knyazikhin, Y., and Park, T.: MODIS/Terra Leaf Area Index/FPAR 8-Day L4 Global 500 m SIN Grid V061 (MOD15A12H.061), NASA EOSDIS Land Processes Distributed Active Archive Center (LP DAAC), https://doi.org/10.5067/MODIS/MODI5A2H.061, 2021.
 - Myneni, R. B., Keeling, C., Tucker, C. J., Asrar, G., and Nemani, R. R.: Increased plant growth in the northern high latitudes from 1981 to 1991, *Nature*, 386, 698–702, https://doi.org/10.1038/386698a0, 1997.
- Peñuelas, J., Poulter, B., Sardans, J., Ciais, P., van der Velde, M., Bopp, L., Boucher, O., Godderis, Y., Hinsinger, P., Llusià, J., Nardin, E., Vicca, S., Obersteiner, M., and Janssens, I. A.: Human-induced nitrogen–phosphorus imbalances alter natural and managed ecosystems across the globe, *Nat. Commun.*, 4, 2934, https://doi.org/10.1038/ncomms3934, 2013.
 Piao, S., Wang, X., Park, T., Chen, C., Lian, X., He, Y., Bjerke, J. W., Chen, A., Ciais, P., Tømmervik, H., Nemani, R. R., and Myneni, R. B.: Characteristics, drivers and feedbacks of global greening, *Nat. Rev. Earth Environ.*, 1, 14–27, https://doi.org/10.1038/s43017-019-0001-x, 2019.
- Prentice, I. C., Bondeau, A., Cramer, W., Harrison, S. P., Hickler, T., Lucht, W., Sitch, S., Smith, B., and Sykes, M. T.: Dynamic global vegetation modeling: Quantifying terrestrial ecosystem responses to large-scale environmental change, in: *Terrestrial Ecosystems in a Changing World*, Springer, Berlin, Heidelberg, 175–192, https://doi.org/10.1007/978-3-540-32730-1 15, 2007.





- 370 Schierhorn, F., Müller, D., Beringer, T., Prishchepov, A. V., Kuemmerle, T., and Balmann, A.: Post-Soviet cropland abandonment and carbon sequestration in European Russia, Ukraine, and Belarus, *Glob. Biogeochem. Cycles*, 27, 1175–1185, https://doi.org/10.1002/2013GB004654, 2013.
 - Sitch, S., O'Sullivan, M., Robertson, E., Friedlingstein, P., Albergel, C., Anthoni, P., Arneth, A., Arora, V. K., Bastos, A., Bastrikov, V., Bellouin, N., Canadell, J. G., Chini, L., Ciais, P., Falk, S., Harris, I., Hurtt, G., Ito, A., Jain, A. K., Jones, M.
- W., Joos, F., Kato, E., Kennedy, D., Klein Goldewijk, K., Kluzek, E., Knauer, J., Lawrence, P. J., Lombardozzi, D., Melton, J. R., Nabel, J. E. M. S., Pan, N., Peylin, P., Pongratz, J., Poulter, B., Rosan, T. M., Sun, Q., Tian, H., Walker, A. P., Weber, U., Yuan, W., Yue, X., and Zaehle, S.: Trends and drivers of terrestrial sources and sinks of carbon dioxide: An overview of the TRENDY project, *Glob. Biogeochem. Cycles*, 38, e2024GB008102, https://doi.org/10.1029/2024GB008102, 2024. Sun, H., Zhang, X., Chen, S., Pei, D., and Liu, C.: Effects of harvest and sowing time on the performance of the rotation of
- 380 winter wheat–summer maize in the North China Plain, *Ind. Crops Prod.*, 25, 239–247, https://doi.org/10.1016/j.indcrop.2006.12.003, 2007.
 - Waha, K., Dietrich, J. P., Portmann, F. T., Siebert, S., Thornton, P. K., Bondeau, A., and Herrero, M.: Multiple cropping systems of the world and the potential for increasing cropping intensity, *Glob. Environ. Change*, 64, 102131, https://doi.org/10.1016/j.gloenvcha.2020.102131, 2020.
- Waha, K., Folberth, C., Biemans, H., Boere, E., Bondeau, A., Hartley, A. J., Hoogenboom, G., Jaegermeyr, J., Liu, Y., Mathison, C., Müller, C., Nkwasa, A., Olin. A., Ruane, A.C., Vos, K.D., White, J.W., Williams, K., and Yu, Q.: Land use modelling needs to better account for multiple cropping to inform pathways for sustainable agriculture, *Commun. Earth Environ*, 6, 756, https://doi.org/10.1038/s43247-025-02724-0, 2025.
- Weatherall, P., Ferreras, S. C., Cardigos, S. D., Cornish, N., Davidson, S. R., Dorschel, B., Drennon, H., Ferrini, V., Harper, H. A., and Isler, T.: The GEBCO_2024 Grid: A continuous terrain model of the global oceans and land, *Earth Syst. Sci. Data*, https://doi.org/10.5194/essd-2024-150, 2024.
 - Wu, W., Yu, Q., You, L., Chen, K., Tang, H., and Liu, J.: Global cropping intensity gaps: Increasing food production without cropland expansion, *Land Use Policy*, 76, 515–525, https://doi.org/10.1016/j.landusepol.2018.03.001, 2018. Xu, L., Myneni, R. B., Chapin III, F. S., Callaghan, T. V., Pinzon, J. E., Tucker, C. J., Zhu, Z., Bi, J., Ciais, P., Tømmervik,
- 395 H., Euskirchen, E. S., Forbes, B. C., Piao, S. L., Anderson, B. T., Ganguly, S., Nemani, R. R., Goetz, S. J., Beck, P. S. A., Bunn, A. G., Cao, C., and Stroeve, J. C.: Temperature and vegetation seasonality diminishment over northern lands, *Nat. Clim. Change*, 3, 581–586, https://doi.org/10.1038/nclimate1836, 2013.
 - Xu, X., Liu, J., and Zhang, S.: China Multi-Period Land Use Remote Sensing Monitoring Dataset (CNLUCC), *National Earth System Science Data Center, China*, http://www.resdc.cn, https://doi.org/10.12078/2018070201, 2018.
- Zhu, Z., Piao, S., Myneni, R. B., Huang, M., Zeng, Z., Canadell, J. G., Ciais, P., Sitch, S., Friedlingstein, P., Arneth, A., Cao, C., Cheng, L., Kato, E., Koven, C., Li, Y., Lian, X., Liu, Y., Liu, R., Mao, J., Pan, Y., Peng, S., Peñuelas, J., Poulter, B., Pugh, T. A. M., Stocker, B. D., Viovy, N., Wang, X., Wang, Y., Xiao, Z., Yang, H., Zaehle, S., and Zeng, N.: Greening of the Earth and its drivers, *Nat. Clim. Change*, 6, 791–795, https://doi.org/10.1038/nclimate3004, 2016.